Peristaltic Flow of a Couple-Stress Fluid with Suspended Nanoparticles in an Asymmetric Channel with Flexible Walls

V. P. Rathod[1] and D. Sanjeevkumar[2*]

[1] *Department of Studies and Research in Mathematics, Gulbarga University, Kalaburagi – 585 106, Karnataka, India.*

[2] *Selection Grade Lecturer Department of Science, Government Polytechnic, Aurad (B), Bidar, Karnataka, India.*

Abstract

An analysis of peristaltic flow of a couple-stress fluid, with immersed nanoparticles, in an asymmetric channel having flexible walls is presented in this paper. General boundary conditions on velocity, temperature and concentration of nanoparticles are used for the analysis. Thermophoresis and Brownian diffusion effects govern the motion of nanoparticles. Long wave length approximation and low Reynolds number assumptions reduce the governing equations of motion into a system of partial differential equations. Closed form solutions for velocity, pressure gradient, pressure rise over a wavelength, temperature distribution and nanoparticle concentration distribution are presented. Effects of slip, couple-stress, thermal and solutal buoyancy, heat exchange, thermophoresis, Brownian motion on velocity profiles, temperature distribution, nanoparticle concentration distribution and pressure rise are discussed. The results of the paper may lead to possible technological applications in the field of biomedicine.

Keywords: *peristaltic motion, asymmetric channel, couple-stress fluid, nano particles, thermophoresis, Brownian motion, slip parameter.*

I. INTRODUCTION

Peristalsis is a process that involves fluid flow in a tubular duct by the waves generated along the wall. Usually one encounters such motion in digestive tract such as the human gastrointestinal tract where smooth muscle tissue contracts and relaxes in sequence to produce a peristaltic wave, which propels the bolus (a ball of food) while in the esophagus and upper gastrointestinal tract, along the tract. The peristaltic movements not only avoid retrograde motion of the bolus but always keep pushing it in the forward direction, i.e., the important aspect of peristalsis is that it can propel the bolus against gravity effectively. Peristaltic movements are effectively used by animals like earthworms and larvae of certain insects (Size 10 & Normal)This document is a template. An electronic copy can be downloaded from the conference website. For questions on paper guidelines, please contact the conference publications committee as indicated on the conference website. Information about final paper submission is available from the conference website. for their locomotion. Motivated by such biomechanisms, there are machineries that imitate peristalsis to cater for specific day-to-day requirements. Other important applications for peristalsis involve, movement of chyme in intestine, movement of eggs in the fallopian tube, transport of the spermatozoa in cervical canal, transport of bile in

the bile duct, circulation of blood in small blood vessels, transport of urine from kidney to urinary bladder and so on.

Over past few decades, peristalsis has attracted much attention of a large class of researchers due to its important engineering and biomedical applications. Following the pioneering work of Latham [1], there have been several reports in literature on the theoretical and experimental studies concerning peristalsis mechanism. Peristaltic flow of Newtonian/non-Newtonian fluids in symmetric channels / axisymmetric tubes has been extensively studied by several authors; Zien and Ostrach [2], Lee and Fung [3], Chaturani and Rathod [4], Srivastava et. al., [5], Takabatake et. al., [6], El Shehawey and Mekheimer [7], Ramachandra and Usha [8], Mekheimer [9], Vajravelu et. al., [10], Mekheimer and Abd elmaboud [11], Rathod and Tanveer [12] and so on. De Vries et. al., [13] have reported that the myometrial contractions may occur not only in symmetric channel but also in an asymmetric channel. With this view point there are quite a lot of studies in the literature related to the peristaltic flow of Newtonian/non-Newtonian fluids in an asymmetric channel; Ramachandra Rao and Mishra [14], Elshehawey, et. al., [15], Subba Reddy et. al., [16], Ali and Hayat [17], Ebaid [18], Sobh [19], Shit et. al., [20], Mekheimer et. al., [21], Srinivas and Muthuraj [22] , Srinivas et. al., [23], Das [24], Abd Elmaboud et. al., [25] and so on.

Current trends in nanotechnology research have lead to wide variety of potential applications in biomedical, optical and electronic engineering, material science, heat transfer engineering and so on. Nanofluid is a homogeneous mixture of particles of nanoscale and carrier fluids like water, ethylene glycol, oil etc., which are commonly known as base fluids. As reported by Choi [26] it is an innovative technique to improve heat transfer by using nanoscale particles in the base fluid. Subsequently, Choi et. al., [27] showed that the addition of a small amount (less than 1% by volume) of nanoparticles to conventional heat transfer fluids increased the thermal conductivity of the fluid up to approximately two times. This innovation has created immense interest in the study of peristaltic flow involving nanofluids in symmetric/asymmetric channels; Akbar and Nadeem [28, 29], Akbar et. al., [30, 31], Mustafa et. al., [32], Beg and Tripathi [33]. It is well known that most of the physiological fluids such as blood behave as a non Newtonian fluid. There are many non-Newtonian fluid models like, power-law model, yield stress power-law model, micropolar model and so on. It is very important to note that the deviation from Newtonian model in case of physiological fluids like blood is mainly due to the suspension of red and white blood cells and platelets in the plasma. The red blood corpuscles are neutrally buoyant in the carrier fluid and there exists a velocity gradient due to shearing stress. These corpuscles undergo rotatory motion and it is also observed that corpuscles possess spin angular momentum, in addition to orbital angular momentum. As a result, the symmetry of stress tensor is lost in the fluid motion that is subjected to spin angular momentum. The fluid that has neutrally buoyant corpuscles, when observed macroscopically, exhibits non-Newtonian behaviour, and its constitutive equation is expressed by a stress tensor as suggested by Stokes [34]. The radius of gyration of the corpuscles for such fluids is different from that of the fluid particles, their difference produces couple stress in the fluid and such fluids are known as couple-stress fluids, in common. The utility of couple-stress fluid model in studies of physiology and biomechanics was suggested by Cowin [35].

In view of the importance of couple-stress fluid model to biomechanics there have been a number of studies concerning peristalsis involving couple-stress fluid, in literature. Srivastava [36] was first amongst others to study peristaltic transport of a couple-stress fluid and broughtout the differences between Newtonian and couple-stress fluid transport. Ali et. al., [37] considered peristaltic flow of a couple stress fluid in an asymmetric channel. Peristaltic flow of a couple stress fluid in an annulus was investigated Mekheimer and Abd Elmaboud [38] and showed that the results have possible endoscopic application. Ranthod and Tanveer [12] investigated the effects of periodic body acceleration and magnetic field on the peristaltic flow of couple-stress fluid through porous medium. Rathod and Asha [39, 40] studied peristaltic transport of a couple stress fluid in a uniform and non uniform annulus with/without an endoscope. Nadeem and Akram [41] investigated the effect of induced magnetic field on the peristaltic flow of a couple stress fluid in an asymmetric channel. Abd Elmabound et. al., [42] studied the thermal properties of couple-stress fluid flow in an asymmetric channel with peristalsis. Studies by Rathod and Sridhar [43] and Rathod and Asha, [44] concern peristaltic transport of couple stress fluid in uniform and non-uniform annulus with and without porous medium, respectively. Rathod et. al., [45] showed that the study of peristaltic pumping of couple stress fluid through a tube with non-erodible porous lining has possible biomedical applications in the treatment of ureter disorders. Raghunath Rao and Prasada Rao [46] studied peristaltic transport of a couple stress fluid permeated with suspended particles. Alsaedi et. al., [47] analysed peristaltic flow of couple stress fluid through uniform porous medium. Shit and Roy [48] considered the hydromagnetic effect on peristaltic flow of a couple-stress fluid through an inclined channel. Recently, Vidhya et. al., [49] considered MHD peristaltic flow of a couple-stress fluid permeated with suspended particles through a porous medium under long wavelength approximation and Hina et. al., [50] reported exact solution for peristaltic flow of couple-stress fluid with wall properties.

Majumder et. al., [51] showed that nanofluidic flow usually exhibits partial slip against the solid surface, which can be characterized by the so-called slip length, which varies in the range 3.4 – 68mm for different liquids. This implies that the slip conditions are the more realistic boundary conditions than the usual no slip boundary conditions. Several authors have considered effect of slip on the peristaltic flow in channels/tubes; Ebaid [18], Shob [19], Das [24] and Akbar et. al., [31]. Recently, Akbar and Nadeem [52] considered both thermal and velocity slip effects on the peristaltic flow of a six-constant-Jeffrey fluid model. Tripathi [53] investigated peristaltic hemodynamic flow of couple-stress fluids through a porous medium with slip effect. Rathod and Kulkarni [54] studied the effect of slip condition and heat transfer in MHD peristaltic transport through a channel filled with porous medium having compliant walls. Rathod and Laxmi [55] studied the slip effect on peristaltic transport of a conducting fluid through a porous medium in an asymmetric vertical channel using Adomian decomposition method. Ebaid and Aly [56] and Rathod and Sanjeevkumar [57] have obtained closed form solutions for peristaltic flow of a nanofluid subjectd to partial slip conditions, without and with magnetic effect, respectively.

In this paper the peristaltic flow of a couple-stress fluid with immersed nanoparticles in an asymmetric channelis to investigated. Thermophoresis and Brownian diffusion effects are considered to

incorporate the behavior of nanoparticlesA attempt is made obtain the closed form solution for the proposed flow, heat and mass transport problem.

II MATHEMATICAL MODEL

consider two dimensional peristaltic transport of an incompressible couple-stress fluid with suspended nanoparticles in an asymmetric channel with flexible walls, generated by propagation of waves on the channel walls travelling with different amplitudes and phases but with constant speed c. In the cartesian coordinates system (x, y), the left wall H_2 and the right wall H_1 are given by (see Figure 1)

$$H_1 = d_1 + a_1 \cos\left[\frac{2\pi}{\lambda}\ x - ct\ \right], \qquad (1)$$

$$H_2 = -d_2 - b_1 \cos\left[\frac{2\pi}{\lambda}\ x - ct\ + \varphi\right]. \qquad (2)$$

Here, a_1 and a_2 are the amplitudes of the waves, λ is the wave length, $d_1 + d_2$ is the width of the channel, φ is the phase difference with the range $0 \le \varphi < \pi$, where $\varphi = 0$ and $\varphi = \pi$ corresponds to symmetric channel with waves out of and in the phase, respectively. It should be noted that the following condition must be achieved

$$a_1^{\,2} + b_1^{\,2} + a_1 b_1 \cos\varphi \le\ d_1 + d_2\ ^2, \qquad (3)$$

with the choice of a_1, b_1, d_1, d_2 and φ, so that the walls will not intersect with each other.

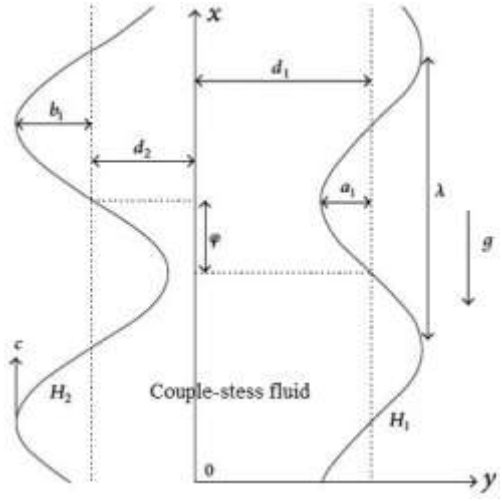

Figure 1. Schematic of the flow configuration.

The conservation equations governing the flow are of the form:

$$\nabla \cdot \mathbf{q} = 0, \qquad (4)$$

$$\rho_f \left(\frac{\partial \mathbf{q}}{\partial t} + \mathbf{q} \cdot \nabla \mathbf{q}\right) = -\nabla p + \mu_f \nabla^2 \mathbf{q} - \eta \nabla^4 \mathbf{q} - \rho_f \left[\alpha\ T - T_0\ + \alpha^*\ S - S_0\ \right] \mathbf{g} \qquad (5)$$

$$\rho C\ _f \left(\frac{\partial T}{\partial t} + \mathbf{q} \cdot \nabla T\right) = k \nabla^2 T + \ \rho C\ _s \left[\left(\frac{D_T}{T_0}\right) \nabla T \nabla T + D_B \nabla S \nabla T\right] \qquad (6)$$

$$\frac{\partial S}{\partial t} + \mathbf{q} \cdot \nabla S = D_B \nabla^2 S + \left(\frac{D_T}{T_0}\right) \nabla^2 T, \qquad (7)$$

where $\mathbf{q} = u, v$ is the velocity vector, u and v are the velocities in x and y directions respectively, p is the pressure, μ_f is the dynamic viscosity coefficient, η couple-stress parameter, $\mathbf{g} = -g, 0$ is gravity vector, ∇^2 is the Laplacian operator, t is the time, ρ_f is the density of the fluid, ρ_s is the density of the nanoparticles, T is the temperature of the fluid, S is the nanoparticle concentration, k is the thermal conductivity, α and α^* are coefficients of thermal

and solutal expansions respectively, C_f and C_s are specific heats at constant pressure of fluid and nanoparticles respectively, T_0 and S_0 are the reference temperature and concentration, D_B is the Brownian diffusion coefficient and D_T is the thermophoretic diffusion coefficient.

The governing equations in component form are given by

$$\frac{\partial u}{\partial x}+\frac{\partial v}{\partial y}=0, \tag{8}$$

$$\rho_f\left(\frac{\partial u}{\partial t}+u\frac{\partial u}{\partial x}+v\frac{\partial u}{\partial y}\right)=-\frac{\partial p}{\partial x}+\mu_f\left(\frac{\partial^2 u}{\partial x^2}+\frac{\partial^2 u}{\partial y^2}\right)$$
$$-\eta\left(\frac{\partial^4 u}{\partial x^4}+2\frac{\partial^2 u}{\partial x^2\partial y^2}+\frac{\partial^4 u}{\partial y^4}\right)+\rho_f\left[\alpha\ T-T_0\ +\alpha^*\ S-S_0\ \right]g, \tag{9}$$

$$\rho_f\left(\frac{\partial v}{\partial t}+u\frac{\partial v}{\partial x}+v\frac{\partial v}{\partial y}\right)=-\frac{\partial p}{\partial y}+\mu_f\left(\frac{\partial^2 v}{\partial x^2}+\frac{\partial^2 v}{\partial y^2}\right)$$
$$-\eta\left(\frac{\partial^4 v}{\partial x^4}+2\frac{\partial^2 v}{\partial x^2\partial y^2}+\frac{\partial^4 v}{\partial y^4}\right) \tag{10}$$

$$\frac{\partial T}{\partial t}+u\frac{\partial T}{\partial x}+v\frac{\partial T}{\partial y}=\frac{k}{\rho C_{\ f}}\left(\frac{\partial^2 T}{\partial x^2}+\frac{\partial^2 T}{\partial y^2}\right)$$
$$+\frac{\rho C_{\ s}}{\rho C_{\ f}}\left[\frac{D_T}{T_0}\left(\frac{\partial T}{\partial y}\right)^2+D_B\frac{\partial S}{\partial y}\frac{\partial T}{\partial y}\right] \tag{11}$$

$$\frac{\partial S}{\partial t}+u\frac{\partial S}{\partial x}+v\frac{\partial S}{\partial y}=D_B\left(\frac{\partial^2 S}{\partial x^2}+\frac{\partial^2 S}{\partial y^2}\right)+\frac{D_T}{T_0}\left(\frac{\partial^2 T}{\partial x^2}+\frac{\partial^2 T}{\partial y^2}\right) \tag{12}$$

Following Shapiro et. al., [3], a wave frame of reference X,Y moving with velocity c is introduced. In this frame the motion becomes independent of time when the channel is an integral multiple of wavelength and pressure difference at the ends of channel is a constant. The transformation from the fixed frame of reference x,y to the wave frame of reference X,Y is given by

$$X=x-ct,\quad Y=y,\quad U=u-c,\quad V=v,$$
$$P\ X,Y\ =p\ x,y,t \tag{13}$$

where U,V are the velocities along coordinate axes in the wave frame and u,v are those in the fixed frame of reference. The pressure $P\ X,Y$ remains constant across any axial station of the channel under the assumption that the wavelength is large and the curvature effects are negligible. Define the following nondimensional variables by:

$$\left.\begin{aligned} &x^*=\frac{2\pi}{\lambda}X,\quad y^*=\frac{Y}{d_1},\quad u^*=\frac{U}{c},\quad v^*=\frac{V}{\delta c},\quad \delta=\frac{2\pi d_1}{\lambda},\\ &p^*=\frac{\delta d_1}{\mu_f c}P, h_1=\frac{H_1}{d_1},\quad h_2=\frac{H_2}{d_1},\quad d=\frac{d_2}{d_1},\quad a=\frac{a_1}{d_1},\\ &b=\frac{b_1}{d_1},\quad \theta=\frac{T-T_0}{T_1-T_0},\quad \phi=\frac{S-S_0}{S_1-S_0}. \end{aligned}\right\} \tag{14}$$

Substituting for new variables from (13) and (14) in equations (8) – (12) and dropping asterisks for simplicity, we get the following equations in the nondimensional form:

$$\frac{\partial u}{\partial x}+\frac{\partial v}{\partial y}=0, \tag{15}$$

$$\delta\,\mathrm{Re}\left(u\frac{\partial u}{\partial x}+v\frac{\partial u}{\partial y}\right)=-\frac{\partial p}{\partial x}+\left(\delta^2\frac{\partial^2 u}{\partial x^2}+\frac{\partial^2 u}{\partial y^2}\right)$$
$$-\frac{1}{Cs^2}\left(\delta^4\frac{\partial^4 u}{\partial x^4}+2\delta^2\frac{\partial^4 u}{\partial x^2\partial y^2}+\frac{\partial^4 u}{\partial y^4}\right)+Gr\theta+Gr^*\phi \tag{16}$$

$$\delta^3\,\mathrm{Re}\left(u\frac{\partial v}{\partial x}+v\frac{\partial v}{\partial y}\right)=-\frac{\partial p}{\partial y}+\delta^2\left(\delta^2\frac{\partial^2 v}{\partial x^2}+\frac{\partial^2 v}{\partial y^2}\right)$$
$$-\frac{\delta^2}{Cs^2}\left(\delta^4\frac{\partial^4 v}{\partial x^4}+2\delta^2\frac{\partial^4 v}{\partial x^2\partial y^2}+\frac{\partial^4 v}{\partial y^4}\right) \tag{17}$$

$$\delta \,\mathrm{Pr}\,\mathrm{Re}\left(u\frac{\partial\theta}{\partial x}+v\frac{\partial\theta}{\partial y}\right)=\delta^2\frac{\partial^2\theta}{\partial x^2}+\frac{\partial^2\theta}{\partial y^2}+Nt\left(\frac{\partial\theta}{\partial y}\right)^2+Nb\frac{\partial\phi}{\partial y}\frac{\partial\theta}{\partial y} \tag{18}$$

$$\delta Sc\,\mathrm{Re}\left(u\frac{\partial\phi}{\partial x}+v\frac{\partial\phi}{\partial y}\right)=\delta^2\frac{\partial^2\phi}{\partial x^2}+\frac{\partial^2\phi}{\partial y^2}+\frac{Nt}{Nb}\left(\delta^2\frac{\partial^2\theta}{\partial x^2}+\frac{\partial^2\theta}{\partial y^2}\right) \tag{19}$$

The nondimensional parameters appearing in equations (16) – (19) are:

$\mathrm{Re}=\dfrac{cd_1}{\upsilon_f}$ the Reynolds number,

$Cs^2=\dfrac{\mu_f d_1^2}{\eta}$ the couple-stress parameter,

$Gr=\dfrac{\rho_f \alpha g\ (T_1-T_0)\ d_1^2}{\mu_f c}$ the thermal Grashof number,

$Gr^*=\dfrac{\rho_f \alpha^* g\ (S_1-S_0)\ d_1^2}{\mu_f c}$ the solutal Grashof number,

$\mathrm{Pr}=\dfrac{\mu C_f}{k}$ the Prandtl number,

$Sc=\dfrac{\upsilon_f}{D_B}$ the Schmidt number

$Nt=\dfrac{\rho C_s D_T\ (T_1-T_0)}{kT_0}$ the thermophoresis parameter,

$Nb=\dfrac{\rho C_s D_B\ (S_1-S_0)}{k}$ the Brownian motion parameter, $\upsilon_f=\dfrac{\mu_f}{\rho_f}$ the kinematic viscosity.

Using stream function $\psi(x,y)$ defined by

$$u=\frac{\partial\psi}{\partial y},\quad v=-\frac{\partial\psi}{\partial x},$$

equation (15) is trivially satisfied and equations (16) – (19), together with long wave length approximation ($\delta \ll 1$) and low Reynolds number limit ($\mathrm{Re} \ll 1$), reduce to the following form:

$$\frac{\partial p}{\partial x}=\frac{\partial^3}{\partial y^3}\left\{\psi-\frac{1}{Cs^2}\frac{\partial^2\psi}{\partial y^2}\right\}+Gr\theta+Gr^*\phi \tag{20}$$

$$\frac{\partial p}{\partial y}=0, \tag{21}$$

$$\frac{\partial^2\theta}{\partial y^2}+Nb\frac{\partial\theta}{\partial y}\frac{\partial\phi}{\partial y}+Nt\left(\frac{\partial\theta}{\partial y}\right)^2=0, \tag{22}$$

$$\frac{\partial^2\phi}{\partial y^2}+\frac{Nt}{Nb}\frac{\partial^2\theta}{\partial y^2}=0. \tag{23}$$

Eliminating pressure from equations (20) and (21) we get

$$\frac{\partial^4}{\partial y^4}\left\{\psi-\frac{1}{Cs^2}\frac{\partial^2\psi}{\partial y^2}\right\}+Gr\frac{\partial\theta}{\partial y}+Gr^*\frac{\partial\phi}{\partial y}=0 \tag{24}$$

The following general boundary conditions are used to solve equations (20) – (24):

$$\psi=\frac{F}{2},\quad \frac{\partial\psi}{\partial y}+\beta\frac{\partial^2\psi}{\partial y^2}=-1,\quad \frac{\partial^3\psi}{\partial y^3}=0 \quad \text{at } y=h_1=1+a\cos x \tag{25}$$

$$\psi=\frac{-F}{2},\quad \frac{\partial\psi}{\partial y}-\beta\frac{\partial^2\psi}{\partial y^2}=-1,\quad \frac{\partial^3\psi}{\partial y^3}=0 \text{ at } y=h_2=-d-b\cos(x+\varphi) \tag{26}$$

$$\theta+Bi\frac{\partial\theta}{\partial y}=0,\ \phi+Bi^*\frac{\partial\phi}{\partial y}=0 \quad \text{at} \quad y=h_1 \tag{27}$$

$$\theta-Bi\frac{\partial\theta}{\partial y}=1,\ \phi-Bi^*\frac{\partial\phi}{\partial y}=1 \quad \text{at} \quad y=h_2 \tag{28}$$

where F is dimensionless time-mean flow rate in the wave frame to be defined in the following subsection, β is the slip parameter, Bi and Bi^* are thermal and solutal Biot numbers respectively.

2.1 Rate of Volume Flow

The instantaneous volume flow rate in the fixed frame is given by

$$q(x,t)=\int_{H_2}^{H_1}u(x,y,t)\,dy, \tag{29}$$

where H_1 and H_2 are given by equations (1) and (2) respectively. The rate of volume flow in the wave frame is given by

$$q^* \ X \ = \int_{H_2}^{H_1} U \ X,Y \ dY \ , \tag{30}$$

where $H_1 = H_1 \ X$ and $H_2 = H_2 \ X$ are functions of X alone. If we substitute (13) into (29) and make use of (30), we find that the two rates of volume flow are related through

$$q \ x,t \ = q^* \ X \ + c\left[H_1 \ x,t \ - H_2 \ x,t \ \right] \tag{31}$$

The time-mean flow over a period T at a fixed position x is defined as

$$q \ x \ = \frac{1}{T}\int_0^T q \ x,t \ dt \ , \tag{32}$$

where, $T = \frac{\lambda}{c}$ is wave period . Now integrating (31) with respect to t over a wave period and using (32) yields the following equation :

$$q \ x \ = q^* \ X \ + c \ d_1 + d_2 \ , \tag{33}$$

On defining the dimensionless time-mean flows Q and F, respectively, in the fixed and wave frame as

$$Q = \frac{q}{d_1 c}, \quad F = \frac{q^*}{d_1 c} \ ,$$

equation (33) may be written as

$$Q = F + 1 + d \ , \tag{34}$$

where $F = \int_{h_2}^{h_1} \frac{\partial \psi}{\partial y} dy = \psi \ h_1 \ - \psi \ h_2 \ \ ,$ which has been used in defining the boundary conditions.

2.2 Pressure rise per wavelength

When the flow is steady in the wave frame, one can characterize the pumping performance by means of the pressure rise per wavelength. The nondimensional pressure rise per wavelength in the wave frame is defined as

$$\Delta P_\lambda = \int_{h_2}^{h_1} \left(\int_0^\lambda \frac{\partial p}{\partial x} dx \right) dy \ . \tag{35}$$

In sections to follow, we present the closed form and perturbation solutions for the energy, species and momentum conservation equations, respectively.

3. Closed form solutions of energy and species equations:

The closed form solutions of the equations (22) – (23) subjected to the boundary conditions (27) – (28) is obtained by integrating equation (23) with respect to y

$$\frac{\partial \phi}{\partial y} = -\frac{Nt}{Nb}\frac{\partial \theta}{\partial y} + f_1(x) \ . \tag{36}$$

Substituting equation (36) in equation (22) we get the following second order differential equation in θ:

$$\frac{\partial^2 \theta}{\partial y^2} + Nbf_1(x)\frac{\partial \theta}{\partial y} = 0 \ . \tag{37}$$

Multiplying equation (37) by $e^{Nbf_1(x)y}$ and integrating with respect to y we get

$$\frac{\partial \theta}{\partial y} = -Nbf_2(x) f_1 \ x \ e^{-Nbf_1(x)y} \ . \tag{38}$$

Integrating equation (38) with respect to y we obtain the solution of the equation (37) as

$$\theta \ x,y \ = f_2(x)e^{-Nbf_1(x)y} + \frac{f_3(x)}{Nb \ f_1(x)} \ . \tag{39}$$

Substituting the solution (39) in equation (36) and integrating the resultant equation with respect to y the solution $\phi \ x,y$ is given by

$$\phi \ x,y \ = -\frac{Nt}{Nb} f_2(x)e^{-Nbf_1(x)y} + f_1(x)y + f_4(x) - \frac{Nt}{Nb^2}\frac{f_3(x)}{f_1(x)} \ , \tag{40}$$

where f_i, $i=1,2,3,4$ are arbitrary functions of x that are to be determined. Using boundary conditions (27) and (28) we get the following relations for f_2, f_3 and f_4 in terms of f_1

$$f_2 = \frac{1}{1+NbBif_1\ e^{-Nbf_1h_2} - 1-NbBif_1\ e^{-Nbf_1h_1}} \tag{41}$$

$$f_3 = \frac{-Nbf_1\ 1-NbBif_1\ e^{-Nbf_1h_1}}{1+NbBif_1\ e^{-Nbf_1h_2} - 1-NbBif_1\ e^{-Nbf_1h_1}} \tag{42}$$

$$f_4 = \frac{Nt}{Nb^2}\frac{f_3}{f_1} + \frac{Nt}{Nb} f_2\ 1-NbBi^*f_1\ e^{-Nbf_1h_1} - h_1 + Bi^*\ f_1 \tag{43}$$

where f_1 satisfies the implicit relation

$$\frac{Nt}{Nb}\left\{\frac{1+NbBi^*f_1\ e^{-Nbf_1h_2} - 1-NbBi^*f_1\ e^{-Nbf_1h_1}}{1+NbBif_1\ e^{-Nbf_1h_2} - 1-NbBif_1\ e^{-Nbf_1h_1}}\right\} . + h_1 - h_2 + 2Bi^*\ f_1 + 1 = 0 \tag{44}$$

4. Closed form solution of momentum equation:

On using the solutions (39) and (40) in equation (24) the solution for $\psi\ x,y$ can be obtained in the form

$$\psi\ x,y\ = g_1(x) + g_2(x)y + g_3(x)y^2 + g_4(x)y^3 + g_5(x)\cosh\ Csy + g_6(x)\sinh\ Csy\ - \frac{Gr^*f_1(x)}{24}y^4 + \frac{Cs^2\bar{G}rf_2(x)e^{-Nbf_1(x)y}}{Nb^4f_1^3(x)\ Nb^2f_1^2(x) - Cs^2}, \tag{45}$$

where $\bar{G}r = GrNb - Gr^*Nt$ and the arbitrary functions $g_i(x)$, $i=1,2,\ldots,6$, on using boundary conditions (25) and (26), can be obtained from the matrix system:

$$\begin{bmatrix} 1 & h_1 & h_1^2 & h_1^3 & \cosh\ Csh_1 & \sinh\ Csh_1 \\ 1 & h_2 & h_2^2 & h_2^3 & \cosh\ Csh_2 & \sinh\ Csh_2 \\ 0 & 1 & 2\ h_1+\beta & 3h_1\ h_1+2\beta & a_{35} & a_{36} \\ 0 & 1 & 2\ h_2-\beta & 3h_2\ h_2-2\beta & a_{45} & a_{46} \\ 0 & 0 & 0 & 0 & Cs^4\cosh\ Csh_1 & Cs^4\sinh\ Csh_1 \\ 0 & 0 & 0 & 0 & Cs^4\cosh\ Csh_2 & Cs^4\sinh\ Csh_2 \end{bmatrix} \begin{bmatrix} g_1(x) \\ g_2(x) \\ g_3(x) \\ g_4(x) \\ g_5(x) \\ g_6(x) \end{bmatrix} = \begin{bmatrix} c_1 \\ c_2 \\ c_3 \\ c_4 \\ c_5 \\ c_6 \end{bmatrix} \tag{46}$$

where,

$$a_{35} = Cs\sinh\ Csh_1\ + \beta Cs^2\cosh\ Csh_1$$

$$a_{36} = Cs\cosh\ Csh_1\ + \beta Cs^2\sinh\ Csh_1$$

$$a_{45} = Cs\sinh\ Csh_2\ - \beta Cs^2\cosh\ Csh_2$$

$$a_{46} = Cs\cosh\ Csh_2\ - \beta Cs^2\sinh\ Csh_2$$

$$c_1 = \frac{F}{2} + \frac{Gr^*f_1}{24}h_1^4 + \frac{Cs^2\bar{G}rf_2e^{-Nbf_1h_1}}{Nb^4f_1^3\ Nb^2f_1^2 - Cs^2}$$

$$c_2 = \frac{-F}{2} + \frac{Gr^*f_1}{24}h_2^4 + \frac{Cs^2\bar{G}rf_2e^{-Nbf_1h_2}}{Nb^4f_1^3\ Nb^2f_1^2 - Cs^2}$$

$$c_3 = -1 + \frac{Gr^*f_1}{6}\ h_1 + 3\beta\ h_1^2 + \frac{Cs^2\bar{G}rf_2\ \beta Nbf_1 - 1\ e^{-Nbf_1h_1}}{Nb^3f_1^2\ Nb^2f_1^2 - Cs^2}$$

$$c_4 = -1 + \frac{Gr^*f_1}{6}\ h_2 - 3\beta\ h_2^2 - \frac{Cs^2\bar{G}rf_2\ \beta Nbf_1 + 1\ e^{-Nbf_1h_2}}{Nb^3f_1^2\ Nb^2f_1^2 - Cs^2}$$

$$c_5 = Gr^*f_1 + \frac{Cs^2\bar{G}rf_1f_2e^{-Nbf_1h_1}}{Nb^2f_1^2 - Cs^2}$$

$$c_6 = Gr^*f_1 + \frac{Cs^2\bar{G}rf_1f_2e^{-Nbf_1h_2}}{Nb^2f_1^2 - Cs^2}.$$

In the following section we present the discussion of the results obtained with the help of analytical solutions obtained so far.

5. Results and discussion

Important results obtained through the exact solutions for the temperature, nanoparticle and velocity distribution and pressure rise over a wavelength is discussed . The results pertaining to the important physical parameters like couple-stress parameter, Grashof numbers, Biot numbers and slip parameters only discussed here as peristaltic flow effect is available in the lirerature. Also, equations (20) - (24) are partially decoupled hence couple-stress and slip parameter affect only velocity distribution and have no effect on the temperature and nanoparticle concentration.

In studying the effect of individual parameters the following fixed values for other parameters are used: a = 0.1, b = 0.5, d = 1, x = 1, φ = 0.2, Nt = 1, Nb = 0.8, Bi = Bi^* = 0.5, F = 5, β = 1, Gr = 1 and Gr^* = 0.5. At this juncture it is to be mentioned that the solutions for velocity, temperature and nanoparticle concentration distribution depend on the arbitrary functions $f_i(x),\ i=1,2,3,4$ and $g_i(x),\ i=1,2,\ldots,6$. The value of the function f_1, for a particular combination of parameter values, is obtained from the implicit relation (44) using Newton – Raphson scheme. Values of other functions can be obtained from equations (41) – (43) and (46). The values of the function f_1 for a given set of parametric values are given in Table 1.

Table1: Values of f_1 for different values of nanoparticle parameters and Biot numbers.

Nt	Nb	Bi	Bi^*	f_1
0	0.8	0.5	0.5	-0.309099
1				-0.695473
2				-1.08185
3				-1.46822
4				-1.85459
5				-2.24097
1	10^{-6}	0.5	0.5	-309099.
	0.2			-1.85459
	0.4			-1.08185
	0.6			-0.824264
	0.8			-0.695473
	1			-0.618198
1	0.8	0	0.5	-0.904464
		1		-0.599906
		2		-0.505285
		3		-0.45751
		4		-0.428532
		5		-0.409049
1	0.8	0.5	0	-0.814386
			1	-0.628793
			2	-0.556941
			3	-0.519029
			4	-0.495642
			5	-0.479785

Figure 2 shows the variation of temperature distribution with respect to thermal and solutal Biot numbers Bi and Bi^* for different values of nanofluid parameters Nt and Nb. It is observed that the temperature increases with the increasing values of the parameters Nt and Nb in both cases of isothermal-isohaline boundary conditions (Bi = Bi^* = 0) and third kind boundary conditions ($Bi \neq 0$ and $Bi^* \neq 0$). At some values of Bi and Bi^* the temperature at the left boundary h_2 increases but for some other values it decreases to take care of the third kind boundary condition. Similar trend is observed at the right boundary h_1 as well. From figure 2 it also observed that in case of clear fluid ($Nt = Nb = 0$) the heat transfer takes place in conduction mode as a result we get linear temperature profiles. Overall, It can say that combined effect of increasing Nt, Nb and Bi, Bi^* leads to irregular pattern in the temperature distribution.

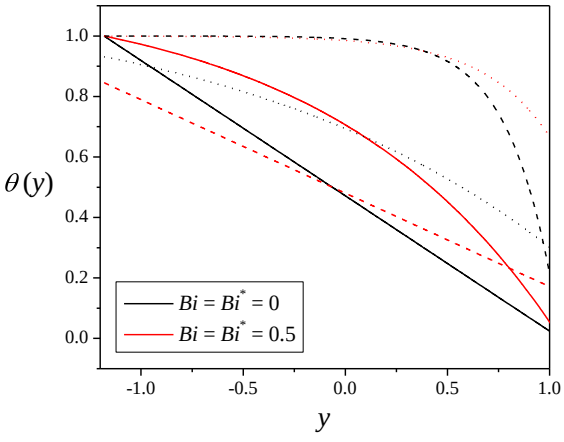

Figure 2. Temperature distribution for different values of Biot numbers

(solid line $Nt = Nb = 10^{-6}$; dashed line $Nt = Nb = 1$; dotted line $Nt = Nb = 5$)

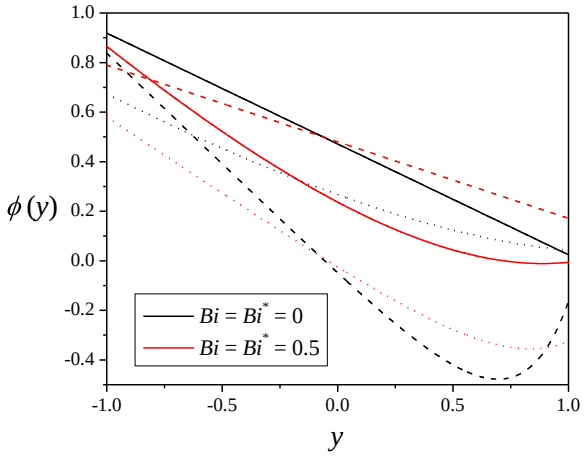

Figure 3. Nanoparticle distribution for different values of Biot numbers

(solid line $Nt = Nb = 10^{-6}$; dashed line $Nt = Nb = 1$; dotted line $Nt = Nb = 5$)

Figure 3 shows the variation of nanoparticle distribution with respect to thermal and solutal Biot numbers Bi and Bi^* for different values of Nt and Nb. From, figure 3 makes out that the concentration of nanoparticles is an increasing function of the parameters Nt and Nb in both cases of isothermal-isohaline boundary conditions (Bi = Bi^* = 0) and third kind boundary conditions ($Bi \neq 0$ and $Bi^* \neq 0$). As observed in the case of temperature distribution, the concentration of nanoparticles at the left boundary h_2 increases for increasing values of Bi and Bi^* and starts decreasing after a point and again it starts increasing. A similar trend follows at right boundary h_1. From figure 3 it also observed that in case of clear fluid (Nt = Nb = 0) the concentration profiles are linear in nature. Overall, it can say that combined effect of increasing Nt, Nb and Bi, Bi^* leads to irregular pattern in the concentration distribution as well.

Now the results concerning couple-stress parameter on the peristaltic flow of fluid with nanoparticle suspensions will be presented. Figure 4 shows the velocity profiles for different values of couple-stress parameter Cs^2 , thermophoresis parameter Nt and Brownian diffusion parameters Nb . From this figure it is seen that, in the absence of nanoparticles, i.e., $Nt \approx 0$ and $Nb \approx 0$, the velocity decreases for increasing values of couple-stress parameter Cs^2 till a critical value, say Cs^{*2} . Further increment in Cs^2 beyond the critical value Cs^{*2} will lead to the opposite effect, i.e., in this regime the velocity increases with increasing values of Cs^2. In the presence of nanoparticles, i.e., $Nt \neq 0$ and $Nb \neq 0$, the velocity increases for increasing values of couple-stress parameter Cs^2 near the walls, where as in the central region it is a decreasing function of Cs^2 . It should be noted that these changes in the velocity are quantitatively very small in the presence of nano-sized particles in a couple-stress fluid. The effect of couple-stress producing suspensions is nullified with the introduction of nano-sized particles. This is due to the fact that the usual suspensions in couple-stress fluid are relatively of grater size than the nanoparticle suspensions and the introduction of such nanoscale particles surrounds the relatively larger couple-stress producing suspensions, giving less chance to inhibit their effect. This may lead to the conclusion that the introduction of nano-sized particles in a couple-stress fluid will render the fluid to behave more or less like a nanofluid.

Figure 5 highlights the effect of couple-stress parameter Cs^2 and slip parameter β on the velocity

profiles. It is observed that increasing values of slip parameter β results in increasing the velocities at both left and right boundaries; the opposite holds in the central region of the channel. In case of no slip condition $\beta = 0$ the velocity profile is more of parabolic in shape and as slip at the walls increases the parabolic profiles starts flattening. This is due to the reason that increasing values of slip parameter β decreases the friction experienced by the fluid at the left and right boundaries, as a result the fluid near boundaries flows at a faster rate thereby reducing the velocity in the interior of the channel. The couple-stress parameter enhances the effect of slip parameter, i.e., near the walls it further increases the velocity and in the central region it further decreases the velocity. From these observations it is infer that the couple-stress fluid slips more than the Newtonian fluid at the walls of the channel.

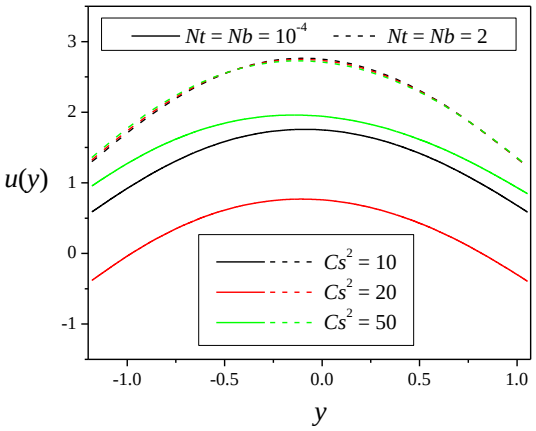

Figure 4. Velocity profiles for different values of couple-stress parameter

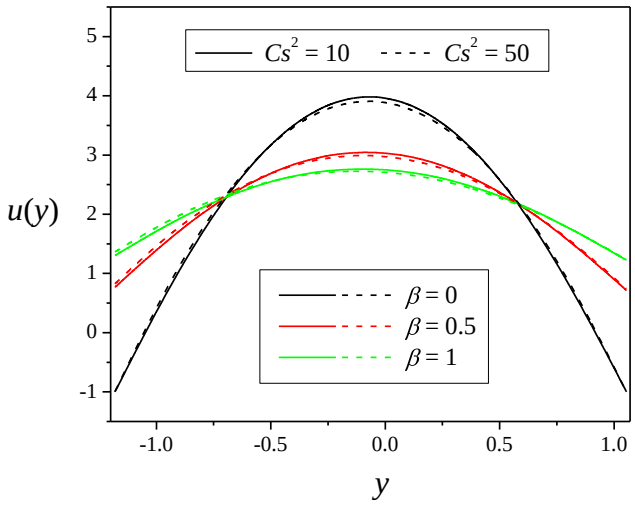

Figure 5. Velocity distribution for different values of slip parameter

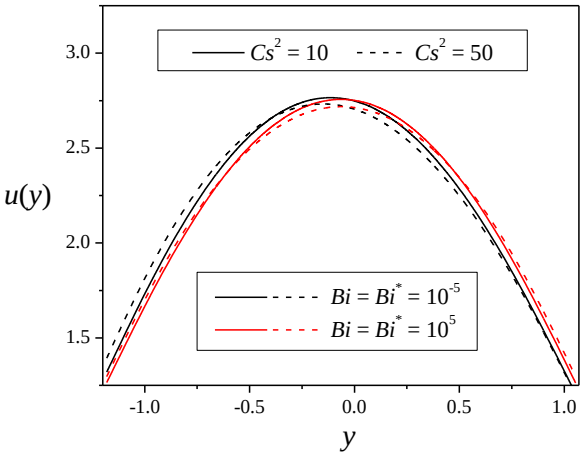

Figure 6. Velocity distribution for different values of Biot numbers

The combined effect couple-stress parameter Cs^2 and the Biot numbers Bi and Bi^* on the velocity profiles is depicted in figure 6. It is evident that, for a given value of couple-stress parameter Cs^2, the velocity near the left wall increases with increasing values of Biot numbers Bi and Bi^* and a mixed effect is observed at the right wall. Further, the maximum velocity decreases with the increasing values of Biot

numbers Bi and Bi^* and shifts from right wall towards the central line of the channel. The couple-stress parameter enhances the effect of Biot numbers, i.e., third kind boundary conditions on temperature and concentration are more appropriate in case of couple-stress fluids.

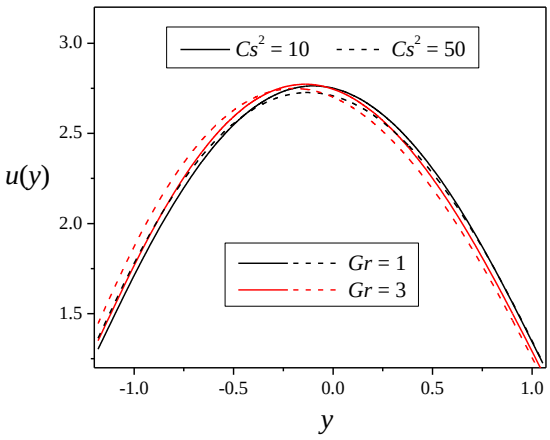

Figure 7. Velocity distribution for different values of thermal Grashof number

The combined effect of couple-stress parameter Cs^2 and the thermal Grashof number Gr is shown in figure 7. It should be noted form figure 7 that, for a given value of couple-stress parameter Cs^2, increasing values of thermal Grashof number Gr results in increasing the velocity in almost the left half of the channel while the opposite trend is recorded in the right half of the channel. At higher values of couple-stress parameter Cs^2, the thermal buoyancy has an opposing effect on the motion of the fluid. Further, the combined action of couple-stress and thermal buoyancy succeeds in pushing the maximum velocity from central region towards the left wall. Figure 8 shows the effect of solutal Grashof number Gr^* for different values of the couple-stress parameter Cs^2 and it is clear that the results of solutal Grashof number Gr^* on the velocity profile is qualitatively similar to that observed in case of thermal Grashof number Gr.

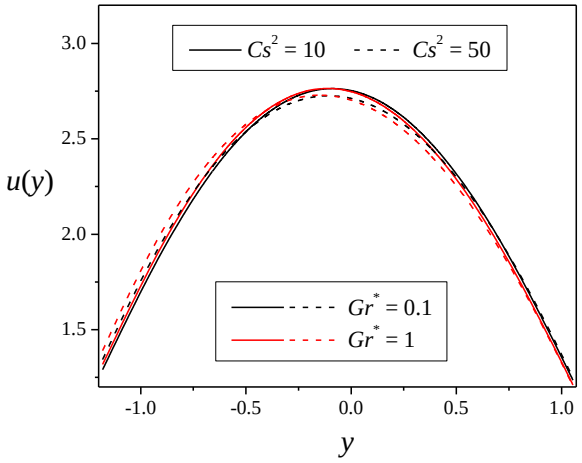

Figure 8. Velocity distribution for different values of solutal Grashof number

Figure 9 indicates the variation of the pressure rise per wavelength ΔP_λ against the time averaged flux Q for different values of couple-stress parameter Cs^2. The time averaged flux Q corresponding to zero pressure rise, i.e., $\Delta P_\lambda = 0$ which is the case of free pumping, by Q^*. The following four sub-regions of the graph are considered:

(i) $\Delta P_\lambda = 0$ and $Q = Q^*$ – the free pumping region,

(ii) $\Delta P_\lambda > 0$ and $Q < 0$ – the backward pumping region,

(iii) $\Delta P_\lambda > 0$ and $Q < Q^*$ – the peristaltic pumping region and

(iv) $\Delta P_\lambda < 0$ and $Q > Q^*$ – the co-pumping region.

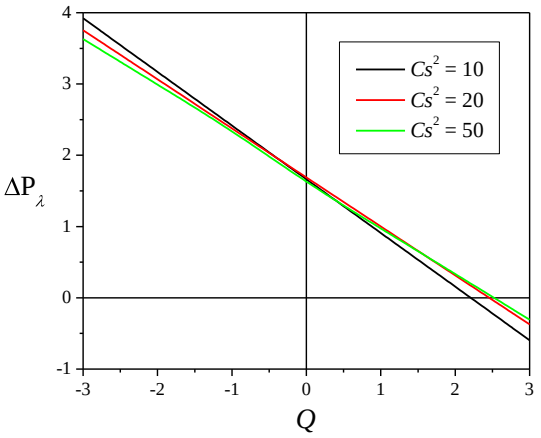

Figure 9. Pressure rise over a wavelength as a function of flow rate for different values of couple-stress parameter

It should be noted the time average flow rate Q^* corresponding to free pumping ($\Delta P_\lambda = 0$) increases with increasing values of couple-stress parameter Cs^2. In general, figure 9 depicts that in the backward pumping region the pressure rise over a wavelength ΔP_λ decreases with increasing values of couple-stress parameter Cs^2. In the peristaltic pumping region the pressure rise over a wavelength ΔP_λ shows a mixed behavior with respect to couple-stress parameter Cs^2 due to the fact that the couple-stress retards the motion till a critical value of Cs^2 is reached and enhances thereafter. In the co-pumping region, the pressure rise over a wavelength ΔP_λ is an increasing function of the couple-stress parameter Cs^2. The mixed behavior in the pressure rise in the peristaltic pumping regime is due to the completion between the usual suspensions and the nano-sized suspensions. For effective biomedical applications one should make sure the concentration of couple-stress producing suspensions should be kept minimum as compared to the concentration of nano-sized suspensions.

6. Conclusions

Analytical solutions for momentum, heat and mass transport in a peristaltic flow of a couple-stress fluid with nanoparticle suspension are obtained subjected to general boundary conditions. Graphical representation of temperature distribution, nanoparticle distribution, velocity distribution and pressure rise over a wavelength for some chosen values of parameters were also presented. The following are few important results of the present analysis:

1. The couple-stress parameter, in the absence of nanoparticle suspensions, has a mixed effect on the velocity of the fluid. The introduction of nanoparticles into couple-stress fluid renders it to behave almost like a nanofluid.
2. The effect of nanofluid parameters on the peristaltic flow is to increase the maximum velocity that shifts from central line towards right wall of the channel. The opposite effect is observed in case of Biot numbers.
3. The couple-stress parameter enhances the slip, thermal and solutal buoyancy effects.
4. The pressure rise in the peristaltic pumping region shows a mixed behavior with respect to the couple-stress parameter.
5. The couple-stress producing suspensions are to be maintained at low concentrations for possible biomedical applications.

References

[1] T. W. Latham, *Fluid motion in a peristaltic pump* [M.S. thesis], MIT, Cambridge, UK, 1966.

[2] T.-F. Zien and S. Ostrach, "A long wave approximation to peristaltic motion," *Journal of Biomechanics*, vol. 3, no. 1, pp. 63–75, 1970.

[3] J.-S. Lee and Y.-C. Fung, "Flow in nonuniform small blood vessels," *Microvascular Research*, vol. 3, no. 3, pp. 272–287, 1971.

[4] P. Chaturani and V. P. Rathod, A theoretical model for pulsatile blood flow with applications to cerebrovascular diseases, Neurological Research 3 (1981) 289-303.

[5] L. M. Srivastava, V. P. Srivastava and S. N. Sinha, "Peristaltic transport of a physiological fluid. Part I. Flow in non-uniform geometry," *Biorheology*, vol. 20, no. 2, pp. 153–166, 1983.

[6] S. Takabatake, K. Ayukawa and A. Mori, "Peristaltic pumping in circular cylindrical tubes: a numerical study of fluid transport and its efficiency," *Journal of Fluid Mechanics*, vol. 193, pp. 267– 283, 1988.

[7] E. F. El Shehawey and K. S. Mekheimer, "Couple-stresses in peristaltic transport of fluids," *Journal of Physics D*, vol. 27, no. 6, pp. 1163–1170, 1994.

[8] R. A. Ramachandra and S. Usha, "Peristaltic transport of two immiscible viscous fluids in a circular tube," *Journal of Fluid Mechanics*, vol. 298, pp. 271–285, 1995.

[9] K. S. Mekheimer, "Peristaltic transport of a couple stress fluid in a uniform and non-uniform channels," *Biorheology*, vol. 39, no.6, pp. 755–765, 2002.

[10] K. Vajravelu, S. Sreenadh and V. R. Babu, "Peristaltic transport of a Herschel-Bulkley fluid in an inclined tube," *International Journal of Non-LinearMechanics*, vol. 40, no. 1, pp. 83–90, 2005.

[11] K. S. Mekheimer and Y. Abd elmaboud, "The influence of heat transfer and magnetic field on peristaltic transport of a Newtonian fluid in a vertical annulus: application of an endoscope," *Physics Letters A*, vol. 372, no. 10, pp. 1657–1665, 2008.

[12] V. P. Rathod and S. Tanveer, Pulsatile flow of couple stress fluid through a porous medium with periodic body acceleration and magnetic Field, Bull. Malays. Math. Sci. Soc. 32 (2) (2009) 245–259.

[13] K. De Vries, E. A. Lyons, G. Ballard, C. S. Levi and D. J. Lindsay, "Contractions of the inner third of themyometrium," *American Journal of Obstetrics and Gynecology*, vol. 162, no. 3,pp. 679–682, 1990.

[14] A. Ramachandra Rao and M. Mishra, Nonlinear and curvature effects on peristaltic flow of a viscous fluid in an asymmetric channel, Acta Mechanica, 168 (2004), 35 - 59.

[15] E. F. Elshehawey, N. T. Eldabe, E. M. Elghazy and A. Ebaid, "Peristaltic transport in an asymmetric channel through a porous medium," *Applied Mathematics and Computation*, vol. 182, no. 1, pp. 140–150, 2006.

[16] M. V. Subba Reddy, A. Ramachandra Rao and S. Sreenadh, "Peristaltic motion of a power-law fluid in an asymmetric channel," *International Journal ofNon-LinearMechanics*, vol. 42, no. 10, pp. 1153–1161, 2007.

[17] N. Ali and T. Hayat, Peristaltic flow of a micropolar fluid in an asymmetric channel. Comput Math Appl, 55 (2008), 589-608.

[18] A. Ebaid, "Effects of magnetic field and wall slip conditions on the peristaltic transport of a Newtonian fluid in an asymmetric channel," *Physics LettersA*, vol. 372, no. 24, pp.4493–4499, 2008.

[19] A. M. Sobh, "Slip flow in peristaltic transport of a Carreau fluid in an asymmetric channel," *Canadian Journal of Physics*, vol. 87, no. 8, pp. 957–965, 2009.

[20] G. C. Shit, M. Roy and E. Y. K. Ng, "Effect of induced magnetic field on peristaltic flow of a micropolar fluid in an asymmetric channel," *International Journal for Numerical Methods in Biomedical Engineering*, vol. 26, no. 11, pp. 1380–1403, 2010.

[21] K. S. Mekheimer, S. Z. A. Husseny and Y. Abd Elmaboud, "Effects of heat transfer and space porosity on peristaltic flow in a vertical asymmetric channel," *Numerical Methods for Partial Differential Equations*, vol. 26, no. 4, pp. 747–770, 2010.

[22] S. Srinivas and R. Muthuraj, "Effects of chemical reaction and space porosity on MHD mixed convective flow in a vertical asymmetric channel with peristalsis," *Mathematical and Computer Modelling*, vol. 54, no. 5-6, pp. 1213–1227, 2011.

[23] S. Srinivas, R. Gayathri and M. Kothandapani, "Mixed convective heat and mass transfer in an asymmetric channel with peristalsis," *Communications in Nonlinear Science and Numerical Simulation*, vol. 16, no. 4, pp. 1845–1862, 2011.

[24] K. Das, "Influence of slip and heat transfer on MHD peristaltic flow of a Jeffrey fluid in an inclined asymmetric porous channel," *Indian Journal of Mathematics*, vol. 54, pp. 19–45, 2012.

[25] Y. Abd Elmaboud, S. Kh. Mekheimer, and A. I. Abdellateef, "Thermal properties of couple-stress fluid flow in an asymmetric channel with peristalsis," *Journal of Heat Transfer*, vol. 135, no. 4, 8 pages, 2013.

[26] S. U. S. Choi, "Enhancing thermal conductivity of fluids with nanoparticles," in *The Proceedings of the ASME International Mechanical Engineering Congress and Exposition*, ASME, San Francisco, Calif, USA. Computational and Mathematical Methods in Medicine

[27] S. U. S. Choi, Z. G. Zhang, W. Yu, F. E. Lockwood, and E. A. Grulke, "Anomalous thermal conductivity enhancement in nanotube suspensions," *Applied Physics Letters*, vol. 79, no. 14, pp. 2252–2254, 2001.

[28] N. S. Akbar and S. Nadeem, "Endoscopic effects on peristaltic flow of a nanofluid," *Communications inTheoretical Physics*, vol. 56, no. 4, pp. 761–768, 2011.

[29] N. S. Akbar and S. Nadeem, "Peristaltic flow of a Phan-Thien-Tanner nanofluid in a diverging tube," *Heat Transfer*, vol. 41, no.1, pp. 10–22, 2012.

[30] N. S. Akbar, S. Nadeem, T. Hayat, and A. A. Hendi, "Peristaltic flow of a nanofluid in a non-uniform tube," *Heat and Mass Transfer/Waerme-und Stoffuebertragung*, vol. 48, no. 2, pp. 451– 459, 2012.

[31] N. S. Akbar, S. Nadeem, T. Hayat, and A. A. Hendi, "Peristaltic flow of a nanofluid with slip effects,"*Meccanica*, vol. 47,pp. 1283–1294, 2012.

[32] M. Mustafa, S.Hina, T.Hayat, and A. Alsaedi, "Influence of wall properties on the peristaltic flow of a nanofluid: analytic and numerical solutions," *International Journal of Heat and Mass Transfer*, vol. 55, pp. 4871–4877, 2012.

[33] O. A. Beg and D. Tripathi, "Mathematica simulation of peristaltic pumping with double-diffusive convection in nanofluids: a bio-nano-engineeringmodel," *Journal of Nanoengineering and Nanosystems*, 2012.

[34] V. K. Stokes, Couple Stresses in Fluids, *Phys* Fluids, vol. 9, pp. 1709-1715, 1966.

[35] S. C. Cowin, The theory of polar fluids. *Advances in Applied Mechanics*, Editor: C.S. Yih, Academic Press, New York, pp. 279-347, 1974.

[36] L. M. Srivastava, Peristaltic transport of couple stress fluid, Rheologica Acta, vol. 25, pp. 638-641, 1986.

[37] N. Ali, T. Hayat and M. Sajid, Peristaltic flow of a couple stress fluid in an asymmetric channel, *Biorheology*, vol. 44(2), pp. 125-38, 2007.

[38] Kh. S. Mekheimer and Y. Abd elmaboud, Peristaltic flow of a couple stress fluid in an annulus: Application of an endoscope, *Physica A: Statistical Mechanics and its Applications*, vol. 387(11), pp. 2403–2415, 2008.

[39] V. P. Rathod and S. K. Asha, Peristaltic transport of a couple stress fluid in a uniform and non uniform annulus, International journal of mathematical modeling ,simulation and application, vol. 2, pp. 414-426, 2009.

[40] V. P. Rathod and S. K. Asha, Effect of couple stress fluid and an endoscope in peristaltic motion, *Ultra Science*, vol. 21, pp. 83–90, 2009.

[41] Sohail Nadeem and Safia Akram, Peristaltic flow of a couple stress fluid under the effect of induced magnetic field in an asymmetric channel, *Archive of Applied Mechanics*, vol. 81 (1), pp. 97-109, 2011.

[42] Y. Abd elmabound, Kh. S. Mekheimer and A. I. Abdellateef, Thermal properties of couple-stress fluid flow in an asymmetric channel with peristalsis, *J. Heat Transfer*, vol. 135(4), art. id. 044502, 2013.

[43] V. P. Rathod and N. G. Sridhar, Peristaltic transport of couple stress fluid in uniform and non-uniform annulus through porous medium, *International Journal of Mathematical Archive*, vol. 3(4), pp. 1561-1574, 2012.

[44] V. P. Rathod and S. K. Asha, Effect of couple stress fluid on peristaltic motion in a uniform and non-uniform annulus, *International Journal of Computer & Organization Trends*, vol. 3(11), pp. 482-490, 2013.

[45] V. P. Rathod, N. G. Sridhar and M. Mahadev, Peristaltic pumping of couple stress fluid through non-erodible porous lining tube wall with thickness of porous material, *Advances in Applied Science Research*, vol. 3 (4), pp. 2326-2336, 2012.

[46] T. Raghunath Rao and D. R. V. Prasada Rao, Peristaltic transport of a couple stress fluid permeated with suspended particles, *International Journal of Advances in Applied Mathematics and Mechanics*, vol. 1(2), pp. 86-102, 2013.

[47] A. Alsaedi, N. Ali, D. Tripathi and T. Hayat , Peristaltic flow of couple stress fluid through uniform porous medium, *Applied Mathematics and Mechanics*, vol. 35(4), pp. 469-480, 2014.

[48] G. C. Shit and M. Roy, Hydromagnetic effect on inclined peristaltic flow of a couple stress fluid, *Alexandria Engineering Journal*, vol. 53, pp. 949–958, 2014.

[49] M. Vidhya, E. P. Siva and A. Govindarajan, MHD peristaltic flow of a couple stress fluid permeated with suspended particles through a porous medium under long wavelength approximation, *ARPN Journal of Engineering and Applied Sciences*, vol. 10(7), pp. 3072-3077, 2015.

[50] S. Hina, M. Mustafa and T. Hayat, On the exact solution for peristaltic flow of couple-stress fluid with wall properties, *Bulgarian Chemical Communications*, vol. 47(1), pp. 30 – 37, 2015.

[51] M. Majumder, N. Chopra, R. Andrews, and B. J. Hinds, "Nanoscale hydrodynamics: enhanced flow in carbon nanotubes," *Nature*, vol. 438, no. 7064, p. 44, 2005.

[52] N.S. Akbar and S. Nadeem, "Thermal and velocity slip effects on the peristaltic flow of a six constant Jeffrey's fluid model," *International Journal of Heat and Mass Transfer*, vol. 55, no. 15-16, pp. 3964–3970, 2012.

[53] Dharmendra Tripathi, Peristaltic hemodynamic flow of couple-stress fluids through a porous medium with slip effect, *Transport in porous media*, vol. 92(3), pp. 559-572, 2012.

[54] V.P. Rathod and Pallavi Kulkarni, The effect of slip condition and heat transfer on MHD peristaltic transport through a porous medium with compliant wall, *Int. J. Applied Mathematical Sciences*, vol. 5, pp. 47-63, 2011.

[55] V. P. Rathod and Laxmi Devindrappa, Slip effect on peristaltic transport of a conducting fluid through a porous medium in an asymmetric vertical channel by Adomian decomposition method, *International Journal of Mathematical Archive*, vol. 4, pp. 133-141, 2013.

[56] A. Ebaid and E.H. Aly, Exact analytical solution of the peristaltic nanofluids flow in an asymmetric channel with flexible walls and slip condition: Application to the cancer treatment, Computational and Mathematical Methods in Medicine, vol. 2013, art. id. 825376, 2013.

[57] V. P. Rathod and D. Sanjeevkumar, Closed form solution of peristaltic flow of a magnetohydrodynamic nanofluid in an asymmetric channel having flexible walls, *International Journal of Mathematical Archive*, vol. 6, no.4, pp. 1-14, 2015.

*** Corresponding author: D. Sanjeevkumar;**

Selection Grade Lecturer Department of Science, Government Polytechnic,Aurad (B), Bidar, Karnataka, India.